

CrystEngComm

Accepted Manuscript



This is an *Accepted Manuscript*, which has been through the Royal Society of Chemistry peer review process and has been accepted for publication.

Accepted Manuscripts are published online shortly after acceptance, before technical editing, formatting and proof reading. Using this free service, authors can make their results available to the community, in citable form, before we publish the edited article. We will replace this *Accepted Manuscript* with the edited and formatted *Advance Article* as soon as it is available.

You can find more information about *Accepted Manuscripts* in the [Information for Authors](#).

Please note that technical editing may introduce minor changes to the text and/or graphics, which may alter content. The journal's standard [Terms & Conditions](#) and the [Ethical guidelines](#) still apply. In no event shall the Royal Society of Chemistry be held responsible for any errors or omissions in this *Accepted Manuscript* or any consequences arising from the use of any information it contains.



Gearing motion in cogwheels pairs of molecular rotors: weak-coupling limit

qReceived 00th January 20xx,
Accepted 00th January 20xx

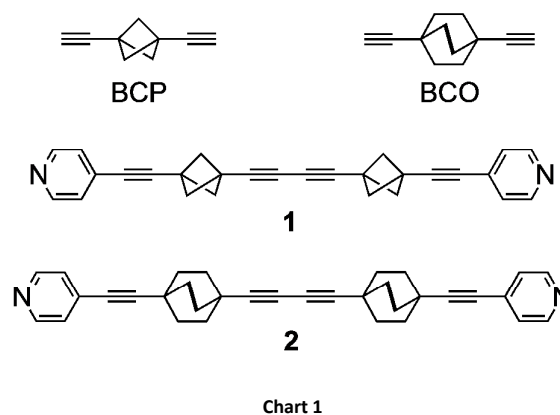
Jiří Kaleta,^a Josef Michl,^{a,b} Cécile Mézière,^c Sergey Simonov,^d Leokadiya Zorina,^d Pawel Wzietek,^e Antonio Rodríguez-Fortea,^f Enric Canadell,^g and Patrick Batail*^c

DOI: 10.1039/x0xx00000x

www.rsc.org/

Variable-temperature (VT) crystal structures, VT ¹H spin-lattice relaxation on static crystals, and DFT modelling of the rotational barriers of the BCP rotators in crystalline arrays of a rod-like molecule containing two 1,3-bis(ethynyl)bicyclo[1.1.1]pentane (BCP) units, demonstrate that a correlated gearing motion occurs in the limit of a weak coupling between two rotors in a pair.

Understanding the mechanism of motion in crystalline arrays of molecular rotors with complex dynamics¹ is a key step that will foster the development of molecular machines capable of performing useful work.^{2–8} The present investigation of the topology and dynamics of solid state assemblies of the rod-like molecule bis(3-(pyrid-4-ylethynyl)bicyclo[1.1.1]pent-1-yl)buta-1,3-diyne, **1** that contains two 1,3-bis(ethynyl)bicyclo[1.1.1]pentane (BCP) rotators linked by a diyne fragment (Chart 1),⁹ was prompted (i) by our recent report¹⁰ of a correlated gearing motion in cogwheel pairs of a similar rod, **2** with 1,4-bis(ethynyl)bicyclo[2.2.2]octane (BCO) rotators⁸ instead; and (ii) the demonstration that, keeping with the one-dimensional topology of **2**, a 4 Å shift of the rotor axles with respect to each other in the thermodynamic polymorph of **2** effectively suppresses the gearing motion.¹¹ Another, yet different, example of correlated rotational motion in a pair is reported here for **1**. The latter is shown to be a structural isomer of **2** where the BCP rotators do not rub against each other as much as the BCO rotators in the kinetic polymorph of **2**, thereby defining a weak-coupling limit for the gearing motion in cogwheel pairs of molecular



rotors.

Self-assembly by C–H⋯N hydrogen bonds in layers of parallel zig-zag strings of rods

The molecular rod **1** was synthesized as reported earlier.⁹ Plate-like colourless crystals were obtained by slow cooling of an ethyl acetate solution and their structure determined by X-ray diffraction at 293 K and 120 K.

As exemplified in Figure 1, a striking feature distinguishes the patterns of self-assembly, and thereby the topologies, of crystalline arrays of **1** and **2**. Instead of two parallel C–H⋯N hydrogen bonds connecting successive rods in **2** into infinite one-dimensional strings, the same two hydrogen bonds (Table S1) connect three rods in **1**, creating infinite zig-zag strings with successive rod axles at an angle of 120° (Fig. 1a), and directing the formation of layers of parallel zig-zag strings of **1** (Fig. 1b). The latter are stacked at a canted angle along *a* (Fig. 1c).

^aInstitute of Organic Chemistry and Biochemistry, Academy of Science of the Czech Republic, Flemingovo nám. 2, 2, 16610 Prague 6

^bDepartment of Chemistry and Biochemistry, University of Colorado, Boulder, CO 80309-0215, United States of America

^cLaboratoire MolTech-Anjou, Université d'Angers, CNRS UMR 6200, 2 Boulevard Lavoisier, 49045 Angers, France

^dInstitute of Solid State Physics RAS, 142432 Chernogolovka MD, Russia

^eLaboratoire de Physique des Solides, Université de Paris-Sud, CNRS UMR 6502, Bâtiment 510, 91405 Orsay, France

^fDepartament de Química Física i Inorgànica, Universitat Rovira i Virgili, Marcel·lí Domingo 1, 43007 Tarragona, Spain

^gInstitut de Ciència de Materials de Barcelona (ICMAB-CSIC), Campus de la UAB, 08193, Bellaterra, Spain.

† Electronic Supplementary Information (ESI) available: Table S1. CCDC 1412010-1412011. For ESI and crystallographic data in CIF see DOI: 10.1039/x0xx00000x

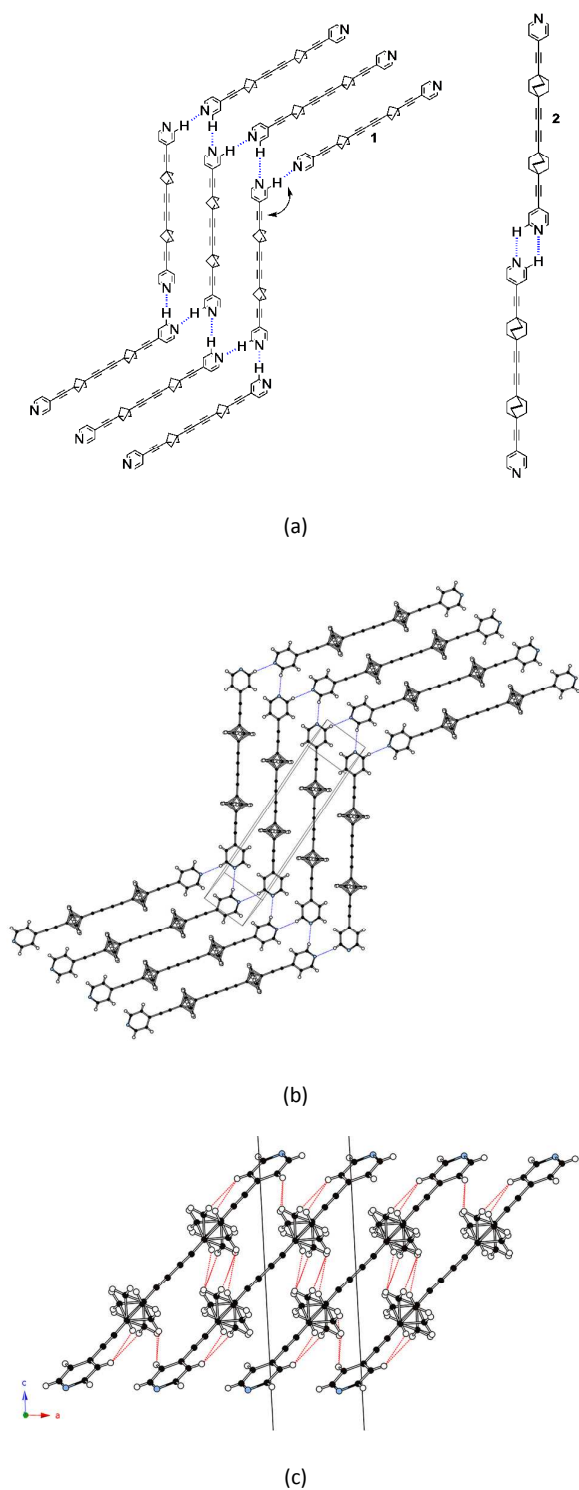


Fig. 1. (a) The two motifs of C-H...N hydrogen bonds in **1** and **2**; (b) A layer of parallel zig-zag strings in **1**; (c) The layers stack at a canting angle along *a*. The dotted red lines are H...H interactions (<2.8 Å) identifying pairs of rotators across layers. Note that the two equilibrium positions are drawn in b and c.

The BCP rotators are located at a single crystallographic site, distributed over two equilibrium positions whose occupancies are unbalanced (0.62 and 0.38 at 293 K; 0.66 and 0.34 at 120 K), yet to

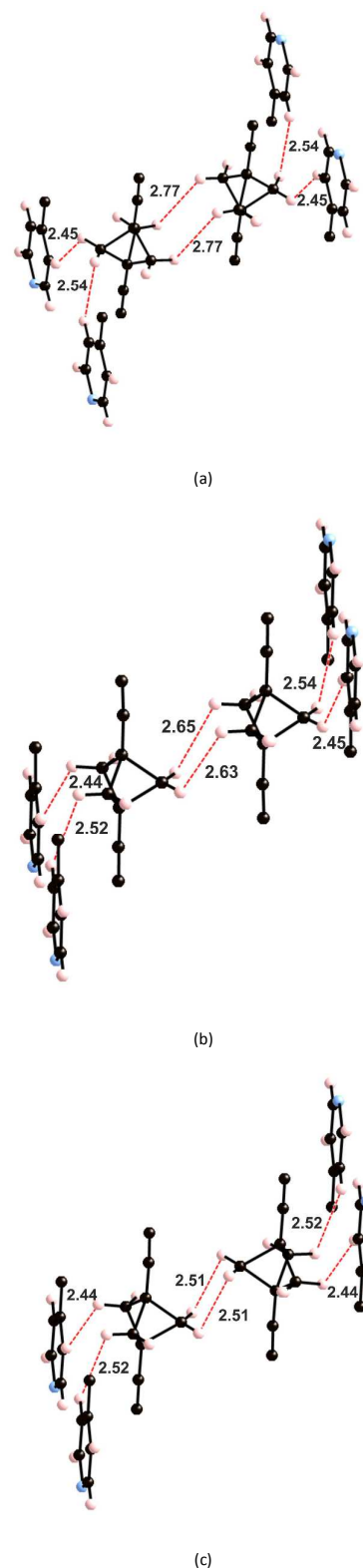


Fig. 2. H...H contacts shorter than 2.8 Å in (a) the Majority-Majority; (b) the Majority-minority and (c) the minority-minority occupancies of the two adjacent rotor sites according to the 120 K structure of **1**.

a lesser extent than in the kinetic polymorph of **2** (0.88 and 0.12 at 293 K).¹⁰ The dotted red lines in Figure 1c show the inventory of H...H interactions shorter than 2.8 Å. It is of interest to note that there is no such contact between BCP rotators in a layer (Fig. 1b). Instead, interacting BCP rotators in a pair are identified in the (*a,c*) plane as a result of stacking the layers along *a* (Fig. 1c). The H...H distances associated with the three possible rotor-rotor interactions corresponding to the occupancies of the two equilibrium positions on a single site, i.e. Majority-Majority (2.770 Å (x2)), minority-minority (2.506 Å (x2)) and Majority-minority (2.630 and 2.650 Å), are shown in Figure 2. In view of such data and our previous work on **2**¹⁰ we anticipate the possibility of two different rotational barriers associated with: (i) a well-correlated *synchronous* motion of the two adjacent rotors and (ii) a higher energy *asynchronous* motion in which two blades of adjacent rotors rub against each other. However there is an important difference between the two systems: whereas in **2** the H...H contacts in the minority-minority situation were as short as 2.1-2.2 Å, in **1** such H...H contacts are kept relatively long. Consequently, the two barriers should be relatively close in the present case.

Variable-temperature ¹H spin-lattice relaxation identifies two relaxation processes

Variable-temperature (35-300 K) proton spin-lattice relaxation experiments were carried out at two fields (with ¹H Larmor frequencies of 46 and 131 MHz) on a static crystalline sample, as described in earlier work.^{8,10-11,12} The correlation time τ_c is obtained by the fit of the ¹H T_1^{-1} data (Fig. 3) to the Kubo-Tomita formula, $\tau_c = \tau_0 \exp(E_a/k_T)$, with two relaxation processes for the same spin temperature to yield rotational barriers of 1.23 kcal mol⁻¹ = 620 K and 1.59 kcal mol⁻¹ = 800 K, and τ_0 of 4.0 10⁻¹³ s and 3.8 10⁻¹³ s, for the low and high energy processes, respectively. The occurrence of two relaxation processes for a rotator with two equilibrium positions with unbalanced occupancies on a single crystallographic site has been observed for the kinetic polymorph of **2** and attributed to the dynamics characteristics of a gearing motion within correlated cogwheels pairs.¹⁰ Note however that in **2**, in

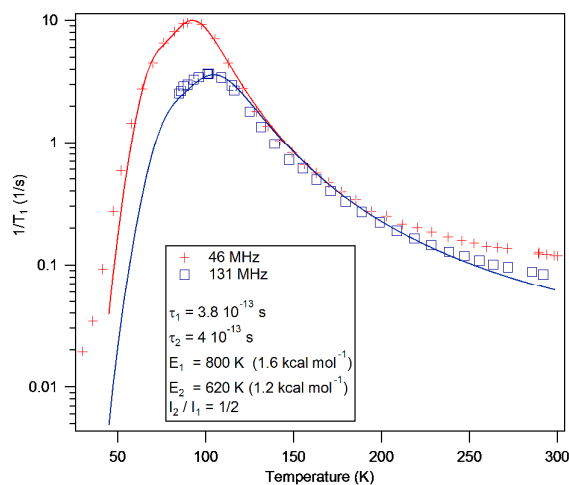


Fig. 3. Variable-temperature proton spin-lattice relaxation time, ¹H T_1^{-1} , at two fields for **1**.

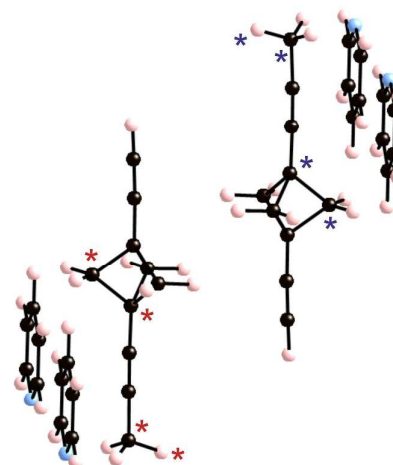


Fig. 4. Model used to study the correlated motion of two adjacent BCP rotators. For the synchronous motion, we fix the dihedral angle θ_1 defined by the atoms labelled by a red asterisk and change it every 10°. For the asynchronous motion, we also fix the dihedral angle defined by the atoms labelled with a blue asterisk (θ_2) at the same value as the θ_1 angle. $\theta = 0^\circ$ corresponds to the dihedral angle of the crystal structure with the majority occupation on the BCP site.

agreement with the analysis above, the energy barriers are typically larger, especially for the high energy process ($E_a = 6.1$ kcal mol⁻¹ = 3078 K).

Modelling the energy barriers

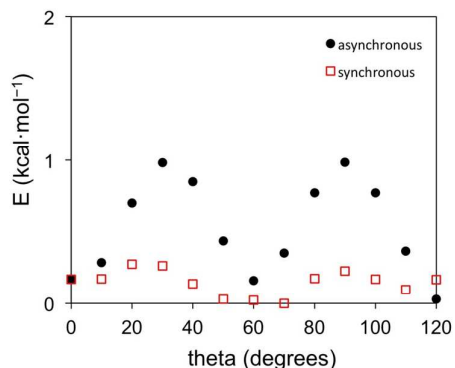
As discussed above (see Fig. 1c) the H atoms of a rotor in **1** are implicated in H...H contacts shorter than 2.8 Å with an adjacent rotor and two pyridine substituents. Consequently, the appropriate model to study the rotational motion in this solid is a couple of neighbouring rotors surrounded with four pyridine fragments, as shown in Figure 4. This model was used in order to estimate the rotational barriers in the solid. The rotors have been modelled as a BCP unit (Chart 1) mimicking the situation in the solid whose triple bonds have been capped in the following manner: 1) by a H atom on the side of the ethynyl group; 2) by a H₃C- on the side of the pyridine. The four neighbouring pyridines, which show relatively short contacts with the blades of the rotors, have been simply considered as pyridine molecules (Figure 2). As in previous studies,^{8,10-11} density functional theory¹³ (DFT) calculations were carried out with the M06-2X functional¹⁴ using the Gaussian 09 code.¹⁵ Basis sets of the type 6-31-G(d,p) were used for C, N and H.¹⁶

We have estimated the two rotational barriers for the synchronous and asynchronous motion of the two BCP rotors in a pair searching for the lowest-energy path by means of partial geometry optimizations. In our calculations, the outer H₃C-C-C- and -C-CH groups of the two rotors are always kept fixed. For the synchronous motion, we fix the dihedral angle (θ_1) defined by the atoms labelled with a red asterisk in Figure 4 and change it every 10°. The coordinates for the two neighbouring rotors have been fully optimized within these restrictions. For the asynchronous

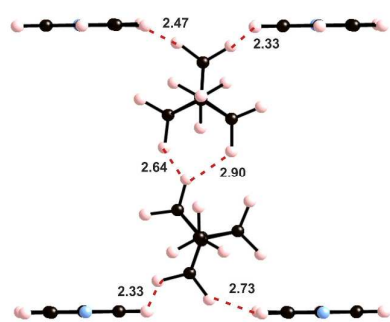
motion, the dihedral angle defined by the atoms labelled with a blue asterisk in Figure 4, were also fixed as the same value of the θ_1 angle. The coordinates of the two rotators have been fully optimized within these restrictions. In both cases the four surrounding pyridine molecules were kept fixed at their crystallographic positions. We have verified that the associated

H...H contacts never become too short and that this assumption is justified.

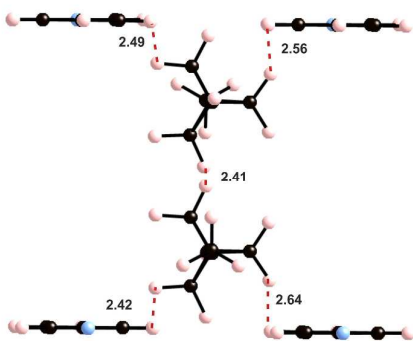
The calculated barriers are reported in Figure 5. That for the synchronous motion is very small, $0.28 \text{ kcal mol}^{-1} = 141 \text{ K}$, whereas that for the asynchronous motion is larger yet not very high, $0.98 \text{ kcal mol}^{-1} = 493 \text{ K}$. These values of the DFT barriers are about 1 kcal mol^{-1} lower than those obtained by the fit of the spin-lattice relaxation data. This is not unexpected in view of such small barriers, particularly since our discrete model does not take into account long-range contributions. The important result is that the energy difference between the two barriers is relatively small in both the spin-lattice relaxation experiments and the DFT calculations. These barriers mostly originate from the variation of the rotor-rotor H...H contacts. The optimized geometries for the higher energy structure of the two types of rotational motions are also shown in Figure 5. It is clear that the rotor-rotor H...H contacts stay considerably long, which is the reason why the barriers are low, as expected. Thus, a picture emerges from this combined experimental and theoretical analysis of the motion of the rotors in a pair where adjacent rotors move gently in a synchronous, well correlated way as long as H...H contacts around 2.4 \AA occurring in the asynchronous motion are avoided, which according to previous work^{10,11} is the onset for the development of repulsive, gear-slipping interactions.



(a)



(b)



(c)

Fig. 5. (a) Computed energy profiles (in kcal mol^{-1}) for the synchronous and asynchronous rotation of two adjacent rotators; (b) Calculated structure of the higher energy structure for the synchronous and (c) asynchronous rotations.

Conclusions

We have shown that the rod-like molecule **1** containing two 1,3-bis(ethynyl)bicyclo[1.1.1]pentane (BCP) rotators, linked by a diyne fragment, self-assembles by C–H...N hydrogen bonds in a crystalline array that proved to be a structural isomer of the analogous rod, **2** carrying 1,4-bis(ethynyl)bicyclo[2.2.2]octane (BCO) rotators instead. As a result, the rod axes are shifted in **1** in such a way that the rotor-rotor interactions defining strong correlated cogwheels pairs in **2** are rather weakened, that is, the rotors do not rub against each other as much in **1**. Our investigation of the rotors dynamics by VT crystal structures and VT spin-lattice relaxation on static crystals, $^1\text{H T}_1^{-1}$, and DFT modelling of the rotational barriers, reveals two low rotational barriers differing by $0.4\text{--}0.7 \text{ kcal mol}^{-1}$, whose energies are rather lower than those in **2** (1.8 and $6.1 \text{ kcal mol}^{-1}$), and concludes that the very same type of correlated gearing motion occurs at thermodynamic equilibrium yet in the limit of a weak coupling between two rotors in a pair, exemplified by a much smaller difference of energy between the low-energy gearing relaxation process and a higher-energy gear-slipping relaxation process.

Acknowledgements

JK and JM gratefully acknowledge financial support from the European Research Council under the European Community's Framework Programme (FP7/2007-2013) ERC grant agreement no 227756 and the Institute of Organic Chemistry and Biochemistry, Academy of Sciences of the Czech Republic

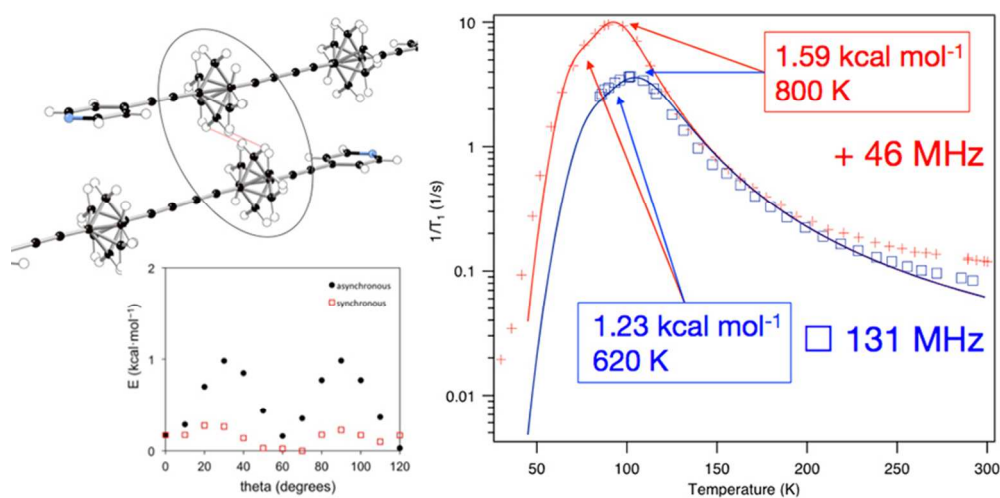
(RVO: 61388963). This material is based upon work supported by the National Science Foundation under Grant No. CHE-1265922. Work at Orsay was supported by the CNRS. Work at Angers was supported by the CNRS, the joint CNRS-Russian Federation grants PICS 6028 and RFBR-CNRS 12-03-91059 (Chernogolovka), and by the Région des Pays de la Loire Grant MOVAMOL. Work in Bellaterra and Tarragona was supported by the Spanish Ministerio de Economía y Competitividad (Projects FIS2012-37549-C05-05 and CTQ2014-52774-P) and Generalitat de Catalunya (2014GR301 and 2014GR199).

Notes and references

† Crystallography. Single crystal X-ray diffraction data were collected with a MoK α (0.71073 Å) radiation on a Bruker Kappa CCD diffractometer at room temperature and with an Oxford Diffraction Gemini-R diffractometer at 120 K (in a cooled nitrogen gas stream). The 293 and 120 K data were processed using the EvalCCD and CrysAlisPro software,¹⁷ respectively; empirical absorption correction were applied with the SADABS and Scale3AbsPack programs.¹⁸ The structure was solved by a direct method followed by Fourier syntheses and refined by a full-matrix least-squares method in an anisotropic approximation for all non-hydrogen atoms using the SHELX-97 programs.¹⁹ H atoms were refined in a riding model with U_{iso}(H) = 1.2 U_{eq}(C). The small thickness of the plate-type crystal and twinning resulted in rather high values of the reliability factors after the structure refinement.

Crystal data for **1** at 293 K: C₂₈H₂₀N₂, M = 384.46, monoclinic P2₁/c, *a* = 5.7123(19), *b* = 5.7076(17), *c* = 33.016(18) Å, β = 93.68(5)°, *V* = 1074.2(8) Å³, *Z* = 2, μ = 0.70 cm⁻¹, 2 θ _{max} = 54.2°, 7162 reflections measured, 2400 unique (*R*_{int} = 0.165), 790 with *I* > 2 σ (*I*), 166 parameters refined, *R*(*F*²) = 0.0769, *wR*(*F*²) = 0.1598, GOF = 0.861. At 120 K: monoclinic P2₁/c, *a* = 5.6780(10), *b* = 5.6456(7), *c* = 32.491(12) Å, β = 93.09(2)°, *V* = 1040.0(4) Å³, *Z* = 2, μ = 0.72 cm⁻¹, 2 θ _{max} = 56.7°, 4203 reflections measured, 2332 unique (*R*_{int} = 0.0617), 1635 with *I* > 2 σ (*I*), 165 parameters refined, *R*(*F*²) = 0.0954, *wR*(*F*²) = 0.2314, GOF = 1.020.

- B. Rodríguez-Molina, S. Peñez-Estrada, and M. A. Garcia-Garibay, M. A., *J. Am. Chem. Soc.*, 2013, **135**, 10388; B. Rodríguez-Molina, N. Farfán, M. Romero, J. M. Méndez-Stivalet, R. Santillan and M. A. Garcia-Garibay, *J. Am. Chem. Soc.* 2011, **133**, 7280; M. A. Garcia-Garibay, *Proc. Natl. Acad. Sci.* 2005, **102**, 10771; T.-A. V. Khuong, J. E. Nunez, C. E. Godinez, and M. A. Garcia-Garibay, *Acc. Chem. Res.*, 2006, **39**, 413; S. D. Karlen, H. Reyes, R. E. Taylor, S. I. Khan, M. F. Hawthorne and M. A. Garcia-Garibay, *Proc. Natl. Acad. Sc. USA*, 2010, **107**, 14973; V. Vogelsberg, M. A. Garcia-Garibay, *Chem. Soc. Rev.*, 2012, **41**, 1892.
- B. L. Feringa, *Acc. Chem. Res.*, 2001, **34**, 504; D. Horinek and J. Michl, *Proc. Natl. Acad. Sci., USA* 2005, **102**, 14175; G. S. Kottas, L. I. Clarke, D. Horinek and J. Michl, *Chem. Rev.*, 2005, **105**, 1281; E. R. Kay, D. A. Leigh and F. Zerbetto, *Angew. Chem. Int. Ed.*, 2007, **46**, 72; K. Skopek, M. C. Hershberger and J. A. Gladysz, *Coord. Chem. Rev.*, 2007, **251**, 1723; L. Kober, K. Zhao, Y. Shen, R. K. Shoemaker, C. T. Rogers and J. Michl, *Cryst. Growth Des.*, 2014, **14**, 559.
- W. Setaka and K. Yamaguchi, *Proc. Natl. Acad. Sc. USA*, 2012, **109**, 9271; W. Setaka and K. Yamaguchi, *J. Am. Chem. Soc.*, 2012, **134**, 17932.
- W. Zhang and R.-G. Xiong, *Chem. Rev.*, 2012, **112**, 1163; W. Zhang, H.-Y. Ye, R. Graf, H. W. Spiess, Y.-F. Yao, R.-Q. Zhu and R.-G. Xiong, *J. Am. Chem. Soc.*, 2013, **135**, 5230.
- S. Horiuchi, Y. Tokunaga, G. Giovanetti, S. Picozzi, H. Itoh, R. Shimano, R. Kumai and Y. Tokura, *Nature*, 2010, **463**, 789; T. Akutagawa, H. Koshinaka, D. Sato, S. Takeda, S. I. Noro, H. Takahashi, R. Kumai, Y. Tokura and T. Nakamura, *Nat. Mater.*, 2009, **8**, 342.
- S. Yamamoto, H. Iida and E. Yashima, *Angew. Chem. Int. Ed.*, 2013, **52**, 6849.
- Q.-C. Zhang, F.-T. Wu, H.-M. Hao, H. Xu, H.-X. Zhao, L.-S. Long, R.-B. Huang and L.-S. Zheng, *Angew. Chem. Int. Ed.*, 2013, **52**, 12602.
- C. Lemouchi, H. M. Yamamoto, R. Kato, S. Simonov, L. Zorina, A. Rodriguez-Fortea, E. Canadell, P. Wzietek, K. Iliopoulos, D. Gindre, M. Chrysos and P. Batail, *Cryst. Growth Des.*, 2014, **14**, 3375; C. Lemouchi, C. S. Vogelsberg, S. Simonov, L. Zorina, P. Batail, S. Brown and M. A. Garcia-Garibay, *J. Am. Chem. Soc.* 2011, **133**, 6371.
- J. Kaleta, P. I. Dron, K. Zhao, Y. Shen, I. Císařová, C. T. Rogers and J. Michl, *J. Org. Chem.*, 2015, **80**, 6173; M. Cipolloni, J. Kaleta, M. Mašát, P. I. Dron, Y. Shen, K. Zhao, C. T. Rogers, R. K. Shoemaker and J. Michl, *J. Phys. Chem. C*, 2015, **119**, 8805; J. Kaleta, M. Nečas and C. Mazal, *Eur. J. Org. Chem.*, 2012, **25**, 4783; J. Kaleta, J. Michl and C. Mazal, *J. Org. Chem.*, 2010, **75**, 2350; C. Mazal, O. Škarka, J. Kaleta and J. Michl, *Org. Lett.*, 2006, **8**, 749; P. F. H. Schwab, B. C. Noll and J. Michl, *J. Org. Chem.*, 2002, **67**, 5476; M. D. Levin, P. Kaszynski and J. Michl, *Chem. Rev.*, 2000, **100**, 169; P. Kaszynski and J. Michl, "[n]Staffanes", in *Advances in Strain in Organic Chemistry, IV*. Halton, B., Ed.; JAI Press Inc., Greenwich, CT, 1995, p. 283; M. D. Levin, S. J. Hamrock, P. Kaszynski, A. B. Shtarev, G. A. Levina, B. C. Noll, M. E. Ashley, R. Newmark, G. G. I. Moore and J. Michl, *J. Am. Chem. Soc.*, 1997, **119**, 12750; A. B. Shtarev, E. Pinkhassik, M. D. Levin, I. Stibor and J. Michl, *J. Am. Chem. Soc.*, 2001, **123**, 3484.
- C. Lemouchi, K. Iliopoulos, L. Zorina, S. Simonov, P. Wzietek, T. Cauchy, A. Rodriguez-Fortea, E. Canadell, J. Kaleta, J. Michl, D. Gindre, M. Chrysos and P. Batail, *J. Am. Chem. Soc.*, 2013, **135**, 9366.
- G. Bastien, C. Lemouchi, M. Allain, P. Wzietek, A. Rodriguez-Fortea, E. Canadell, K. Iliopoulos, D. Gindre, M. Chrysos and P. Batail, *CrystEngComm*, 2014, **16**, 1241.
- See also: A. Comotti, S. Bracco, T. Ben, S. Qiu and P. Sozzani, *Angew. Chem. Int. Ed.*, 2014, **53**, 1043; A. Comotti, S. Bracco, A. Yamamoto, M. Beretta, T. Hirukawa, N. Tohnai, M. Miyata and P. Sozzani, *J. Am. Chem. Soc.*, 2014, **136**, 618.
- P. Hohenberg and W. Kohn, *Phys. Rev.* 1964, **136**, B864; W. Kohn and L. J. Sham, *Phys. Rev.*, 1965, **140**, A1133.
- Y. Zhao and D. G. Truhlar, *Theo. Chem. Acc.*, 2008, **120**, 215.
- Gaussian 09, Revision B1, M. J. Frisch, G. W. Trucks, H. B. Schlegel, G. E. Scuseria, M. A. Robb, J. R. Cheeseman, G. Scalmani, V. Barone, B. Mennucci, G. A. Petersson, H. Nakatsuji, M. Caricato, X. Li, H. P. Hratchian, A. F. Izmaylov, J. Bloino, G. Zheng, J. L. Sonnenberg, M. Hada, M. Ehara, K. Toyota, R. Fukuda, J. Hasegawa, M. Ishida, T. Nakajima, Y. Honda, O. Kitao, H. Nakai, T. Vreven, J. A. Montgomery Jr., J. E. Peralta, F. Ogliaro, M. Bearpark, J. J. Heyd, E. Brothers, K. N. Kudin, V. N. Staroverov, R. Kobayashi, J. Normand, K. Raghavachari, A. Rendell, J. C. Burant, S. S. Iyengar, J. Tomasi, M. Cossi, N. Rega, J. M. Millam, M. Klene, J. E. Knox, J. B. Cross, V. Bakken, C. Adamo, J. Jaramillo, R. Gomperts, R. E. Stratmann, O. Yazyev, A. J. Austin, R. Cammi, C. Pomelli, J. W. Ochterski, R. L. Martin, K. Morokuma, V. G. Zakrzewski, G. A. Voth, P. Salvador, J. J. Dannenberg, S. Dapprich, A. D. Daniels, Ö Farkas, J. B. Foresman, J. V. Ortiz, J. Cioslowski and D. J. Fox, Gaussian Inc., Wallingford CT, 2009.
- R. Krishnan, J. S. Binkley, R. Seeger and J. A. Pople, *J. Chem. Phys.*, 1980, **72**, 650.
- A. J. M. Duisenberg, L. M. J. Kroon-Batenburg and A. M. M. Schreurs, *J. Appl. Crystallogr.*, 2003, **36**, 220; CrysAlisPro, Agilent Technologies, Version 1.171.37.34c.
- G. M. Sheldrick, SADABS, University of Göttingen, Germany, 1996; SCALE3ABSPACK, Agilent Technologies, Version 1.171.37.34c.
- G. M. Sheldrick, *Acta Crystallogr., Sect. A: Found. Crystallogr.* 2008, **64**, 112.



Investigation of the rotor dynamics by VT crystal structures, VT spin-lattice relaxation on static crystals, and DFT modelling of the rotational barriers in crystalline arrays of a self-assembled rod-like molecule containing two 1,3-bis(ethynyl)bicyclo[1.1.1]pentane (BCP) rotators reveals two low rotational barriers and conclude that correlated gearing motion occurs at thermodynamic equilibrium in the limit of a weak coupling between two rotors in a pair.

77x39mm (300 x 300 DPI)